

Electronic Supplementary Information (ESI)

Diverse dissolution-recrystallization structural transformations and sequential Förster resonance energy transfer behavior of a luminescent porous Cd-MOF

Li-Hui Cao,^{a,b} Hai-Yang Li,^a Hong Xu,^a Yong-Li Wei^{*,a} and Shuang-Quan Zang^{*,a}

^a College of Chemistry and Molecular Engineering, Zhengzhou University, Zhengzhou 450001, China

^b College of Chemistry and Chemical Engineering, Shaanxi University of Science & Technology, Xi'an 710021, China

*E-mail: zangsqz@zzu.edu.cn, weiyongli@zzu.edu.cn

Table of Contents

Section S1: Single Crystal X-ray Diffraction Analyses	S2-S8
Section S2: Powder X-ray Diffraction Patterns	S9-S10
Section S3: Thermal Gravimetric Analyses	S11
Section S4: Fluorescent Characteristics	S12
Section S5: Supplementary References	S14

Section S1: Single Crystal X-ray Diffraction Analyses

Single-crystal X-ray diffraction data were collected on a Bruker SMART APEX CCD diffractometer^[S1] equipped with a graphite-monochromated Mo-K α radiation ($\lambda = 0.71073$ Å) at 100 K or 293 K using the ω -scan technique. Data reduction was performed using SAINT and corrected for Lorentz and polarization effects. Adsorption corrections were applied using the SADABS routine.^[S2] All the structures were solved with direct methods (*SHELXS*)^[S3] and refined by full-matrix least squares on F^2 using *OLEX2*,^[S4] which utilizes the *SHELXL-2015* module.^[S5] All non-hydrogen atoms were refined anisotropically. Geometrical restraints were used in modeling the disordered amine groups. Displacement parameter restraints were used in modeling the ligands and solvent molecules. Hydrogen atoms were placed geometrically on their riding atom where possible. Complex **1**, which is racemic, belongs to the trigonal space group *P3*. It is a pity that we cannot obtain the pure chiral complex. For the data of complex **1**, the diffuse electron densities resulting from the residual solvent molecules were removed from the data set using the SQUEEZE routine of PLATON and refined further using the data generated.^[S6] The contents of the solvent region are not represented in the unit cell contents in the crystal data. Crystal data containing space group, lattice parameters and other relevant information for the title compound are summarized in Table S1. More details on the crystallographic data are given in the X-ray crystallographic files in CIF format.

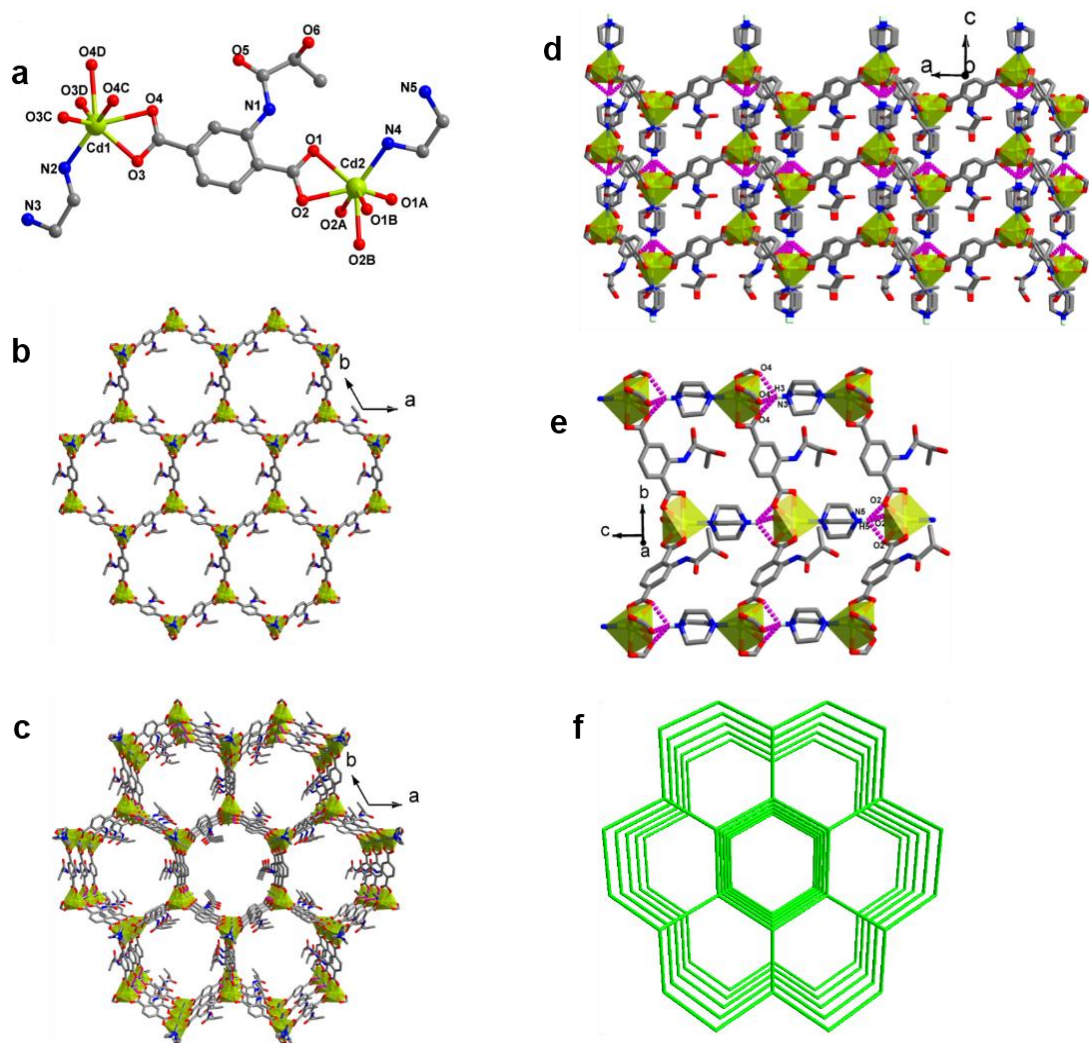


Fig. S1 (a) Coordination environment of Cd^{2+} in complex **1**. Symmetry codes: A $1 - y, x - y, z$; B $1 - x + y, 1 - x, z$; C $-y, x - y, z$; D $-x + y, -x, z$. (b) 2D structure in complex **1**. (c) and (d) View from different directions of the 3D supramolecular network. (e) The N–H \cdots O hydrogen bonding interactions are presented by broken pink lines: $\text{N3} \cdots \text{O4} = 2.888 \text{ \AA}$; $\text{N5} \cdots \text{O2} = 2.840 \text{ \AA}$. (f) Schematic view of the uninodal net.

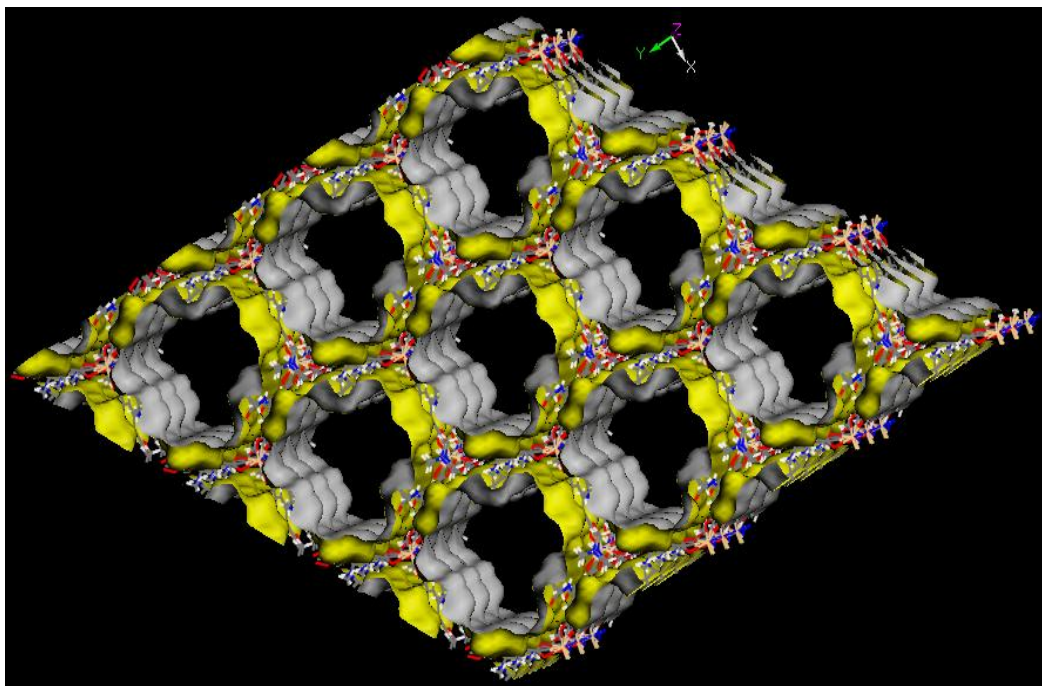


Fig. S2 Nanochannels of complex **1** viewed along the c -axis, where the yellow surface represents the pore surface.

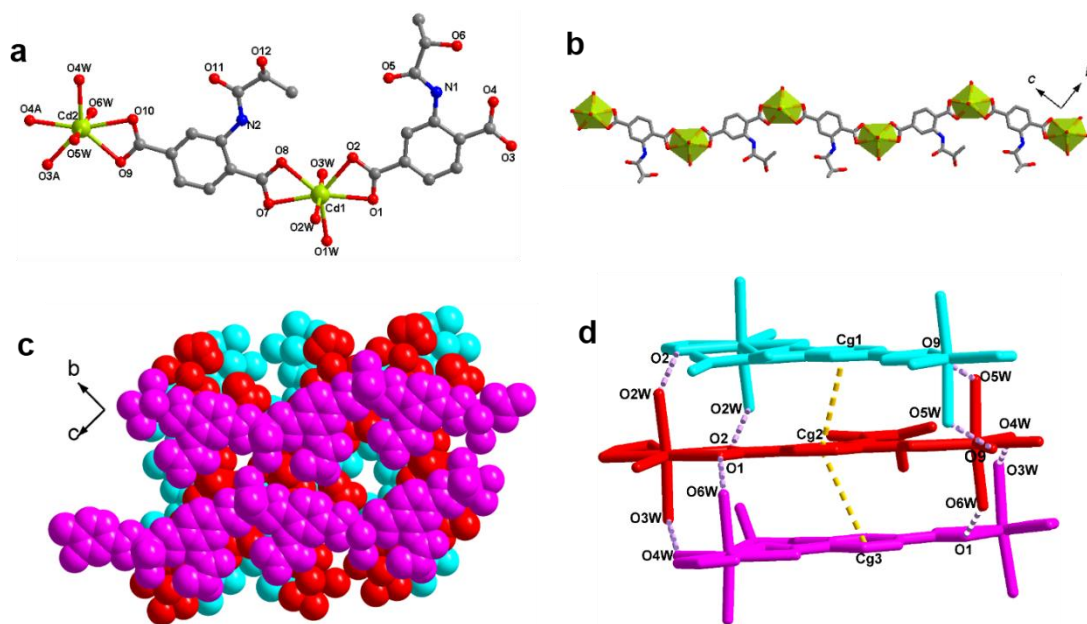


Fig. S3 (a) Coordination environment of Cd²⁺ in complex **2**. Symmetry codes: A $x, -1 + y, 1 + z$. (b) 1D structure in complex **2**. (c) A space-filling view of the 3D supramolecular structure. (d) The $\pi \cdots \pi$ and O–H \cdots O hydrogen bonding interactions are presented by broken gold and pink lines, respectively. The distances between adjacent benzene rings were 3.742 Å (Cg1 \cdots Cg2) and 3.677 Å (Cg2 \cdots Cg3). The distances between adjacent oxygen atoms having hydrogen bonding: O2W \cdots O2 = 2.673 Å; O3W \cdots O4W = 2.703 Å; O5W \cdots O9 = 2.639 Å; O6W \cdots O1 = 2.642 Å;.

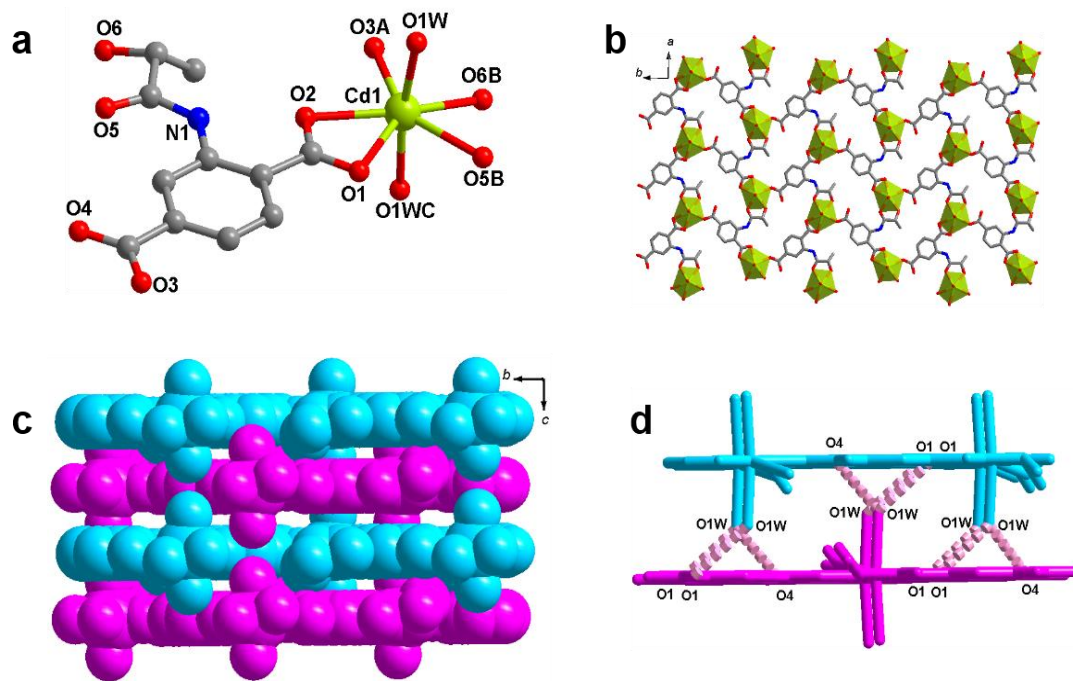


Fig. S4 (a) Coordination environment of Cd^{2+} in complex **3**. Symmetry codes: A $1 - x, 0.5 + y, 0.5 - z$; B $1 + x, y, z$; C $x, y, 0.5 - z$. (b) 2D structure in complex **3**. (c) A space-filling view of the 3D supramolecular structure. (d) The hydrogen bonding interactions are presented by broken rose lines: $\text{O1} \cdots \text{O1W} = 2.790 \text{ \AA}$; $\text{O4} \cdots \text{O1W} = 2.779 \text{ \AA}$.

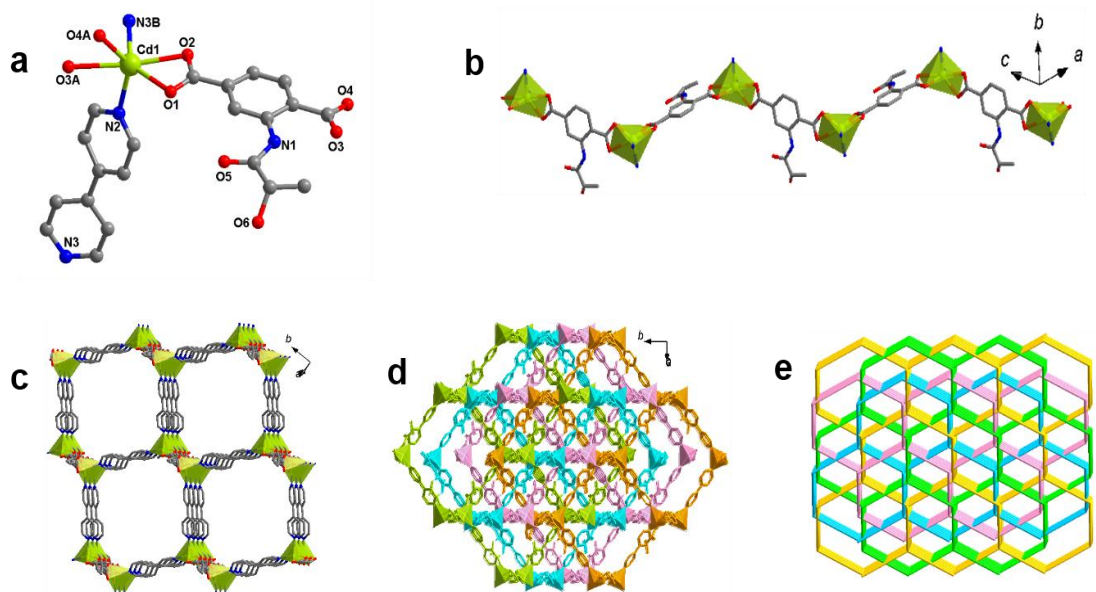


Fig. S5 (a) Coordination environment of Cd^{2+} in complex **4**. Symmetry codes: A $-0.5 + x, 1.5 - y, 0.5 + z$; B $0.5 + x, 2.5 - y, 0.5 + z$. (b) wavy chain structure created by L_1^{2-} ligands and Cd^{2+} ions. (c) 3D latticed construction created by L_1^{2-} ligands, adscitious bpy and Cd^{2+} ions. (d) 4-fold interpenetrating framework of complex **4**. (e) Schematic view of the 4-fold interpenetration structure.

Table S1: Crystal structure and refinement details of complexes **1-4**.

Complexes	1	2	3	4
Empirical formula	C ₄₅ H ₅₃ Cd ₂ N ₇ O ₁₈	C ₂₂ H ₃₂ Cd ₂ N ₂ O ₁₉	C ₁₁ H ₁₃ CdNO ₈	C ₂₁ H ₁₉ CdN ₃ O ₇
Formula weight	1204.74	853.29	399.62	537.79
Temperature / K	100.00	99.95	294.36	299.57
Wavelength / Å	0.71073	1.54178	0.71073	0.71073
Crystal system	trigonal	monoclinic	orthorhombic	monoclinic
Space group	<i>P</i> 3	<i>P</i> 2/ <i>c</i>	<i>Pbcm</i>	<i>P</i> 2 ₁ / <i>c</i>
<i>a</i> / Å	17.9750(14)	14.0033(4)	9.1904(3)	13.199(2)
<i>b</i> / Å	17.9750(14)	13.5730(3)	18.4142(7)	11.715(3)
<i>c</i> / Å	8.8636(4)	16.4628(4)	7.9980(3)	14.375(4)
<i>α</i> / °	90	90	90	90
<i>β</i> / °	90	95.083(2)	90	98.15(2)
<i>γ</i> / °	120	90	90	90
Volume / Å ³	2480.1(4)	3116.73(14)	1353.53(8)	2200.4(8)
<i>Z</i>	1	4	4	4
Density (calculated) / g cm ⁻³	0.807	1.818	1.961	1.623
Absorption coefficient / mm ⁻¹	0.469	11.694	1.653	1.040
F(000)	612	1704	792	1080
Reflections collected	5364	24275	15911	14106
Independent reflections	4046	5169	1507	3843
Data / restraints / parameters	4046 / 175 / 207	5169 / 82 / 415	1507 / 46 / 129	3843 / 96 / 291
Goodness-of-fit on <i>F</i> ²	1.001	1.084	1.055	1.080
^a <i>R</i> ₁ , ^b <i>wR</i> ₂ [<i>I</i> > 2σ(<i>I</i>)]	0.0524, 0.0978	0.0724, 0.2067	0.0353, 0.0902	0.0597, 0.1536
^a <i>R</i> ₁ , ^b <i>wR</i> ₂ (all data)	0.0666, 0.0988	0.0859, 0.2165	0.0439, 0.0942	0.0871, 0.1642
Largest diff. peak and hole / e.Å ⁻³	1.31 / -0.56	2.33 / -1.01	1.40 / -1.13	1.15 / -0.58

$${}^a R_1 = \sum ||F_o| - |F_c|| / \sum |F_o|. \quad {}^b wR_2 = [\sum w(F_o^2 - F_c^2)^2 / \sum w(F_o^2)]^{1/2}.$$

Section S2: Powder X-ray Diffraction Patterns

The bulk-phase purity of all afore-mentioned materials was confirmed by comparison of recorded powder X-ray diffraction (PXRD) patterns with simulated patterns from single-crystal data. All PXRD peaks of as-synthesized complex **1** to complex **4** matched exactly with the respective simulated patterns (see Fig. S6).

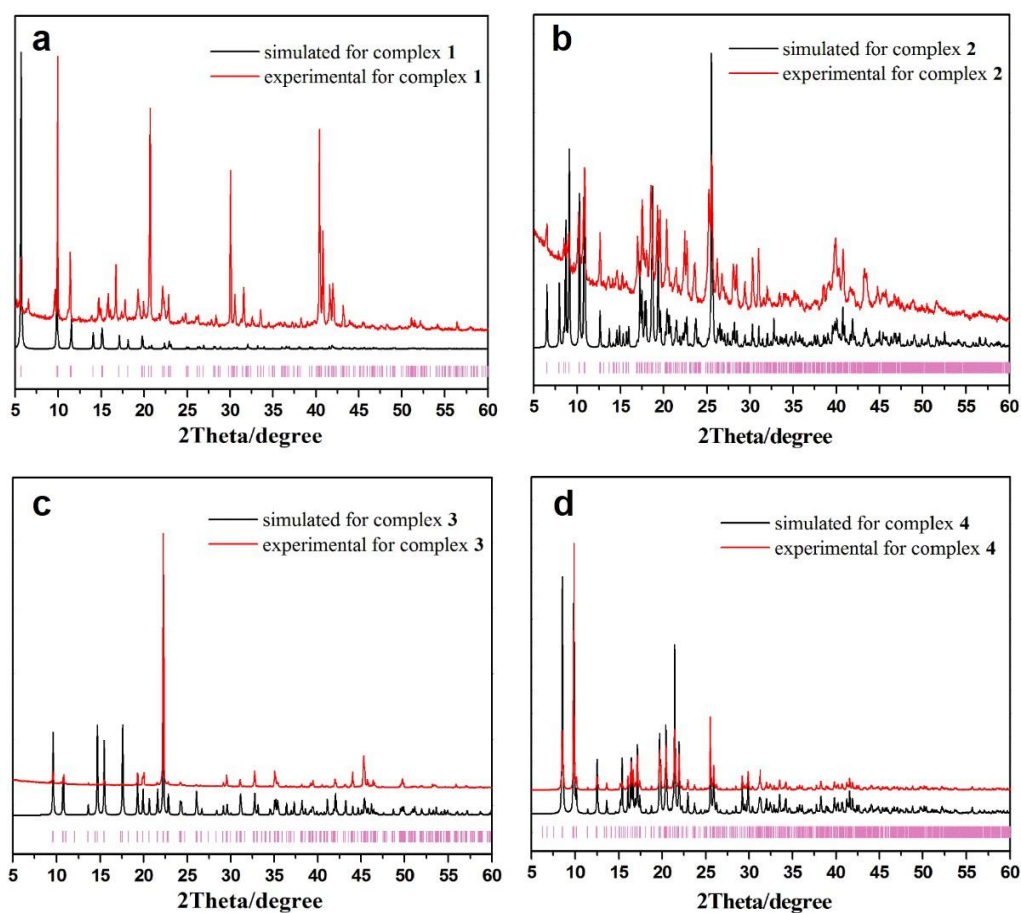


Fig. S6 The simulated and experimental PXRD patterns of complexes **1-4**.

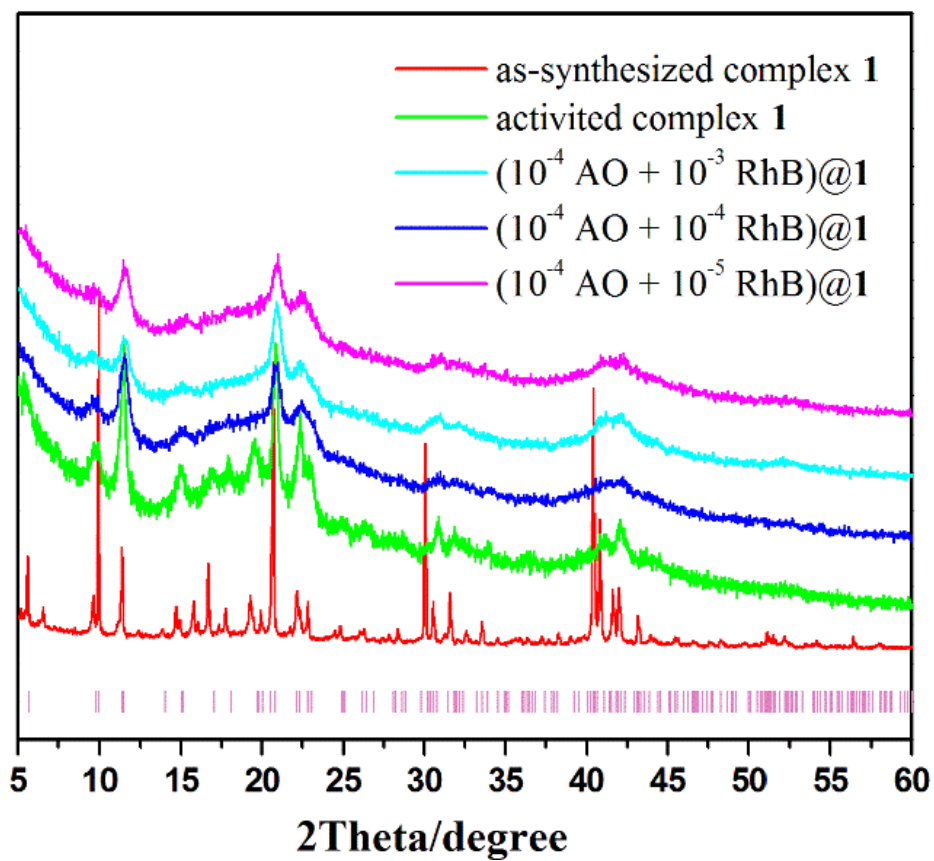


Fig. S7 PXRD patterns of before and after loading dyes.

Section S3: Thermal Gravimetric Analyses

To study the thermal stability of these coordination polymers, thermogravimetric analysis (TGA) were performed (Fig. S8). For complexes **1-4**, weight loss between 30 and 150 °C is attributed to the release of solvated and coordinated water molecules, and the organic solvents began to lose gradually between 150 to 230 °C. Rapid weight losses were observed from 290 °C, which indicated collapse of the whole structure.

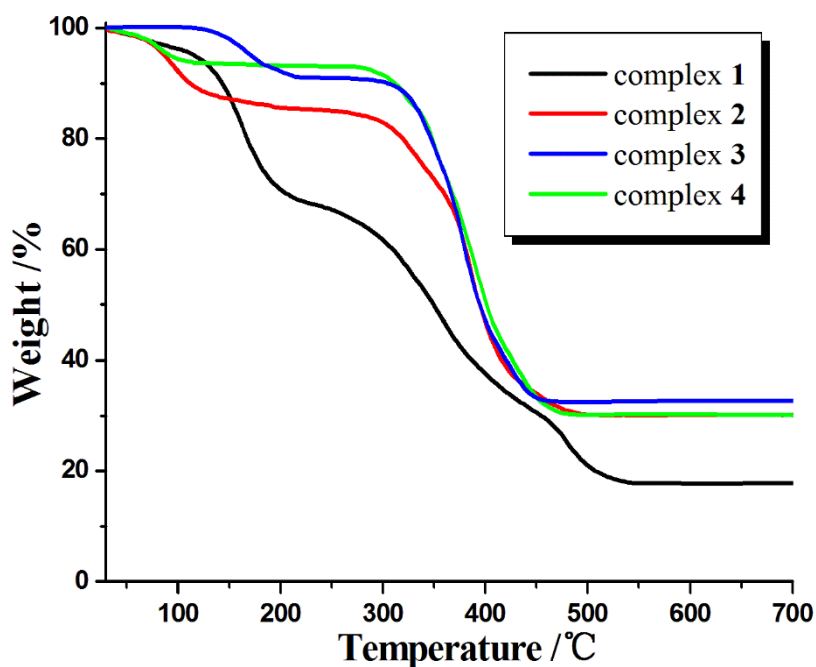


Fig. S8 TGA results of complexes **1-4**.

Section S4: Fluorescent Characteristics

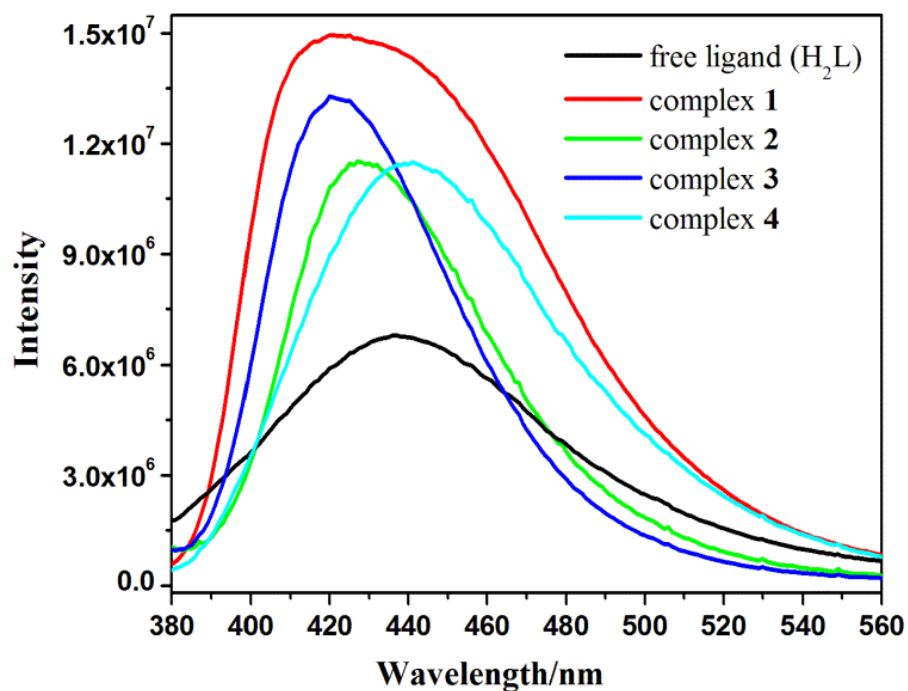


Fig. S9 Solid-state emission spectra of free ligand and complexes **1–4** at room temperature.

Table S2: Fluorescence lifetime and quantum yield of excited states.

Emission peak		420 nm	532 nm	606 nm
complex 1	lifetime/ns	4.05	/	/
	quantum yield (QY)/%	11.08	/	/
AO@ 1	lifetime/ns	2.64	4.95	/
	quantum yield (QY)/%	1.71	48.25	/
(AO+RhB)@ 1	lifetime/ns	2.07	3.82	5.69
	quantum yield (QY)/%	3.20	1.15	27.17

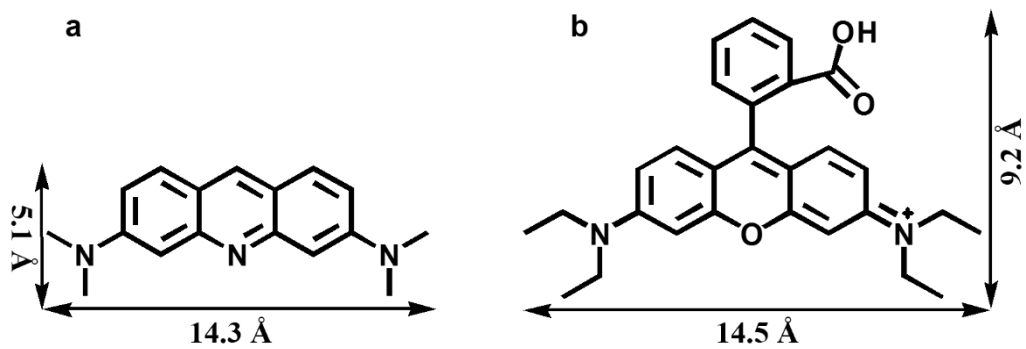


Fig. S10 Molecular structures and sizes of (a) acridine orange (AO), (b) rhodamine B (RhB).

Section S5: Supplementary References

- [S1] *SMART and SAINT. Area Detector Control and Integration Software*; Siemens Analytical X-Ray Systems, Inc.: Madison, WI, 1996.
- [S2] G. M. Sheldrick, *SADABS: Program for Empirical Absorption Correction of Area Detector Data*, University of Göttingen, Germany, 1996.
- [S3] G. M. Sheldrick, *Acta Cryst. A*, 2008, **64**, 112.
- [S4] O. V. Dolomanov, L. J. Bourhis, R. J. Gildea, J. A. K. Howard and H. Puschmann, *J. Appl. Cryst.*, 2009, **42**, 339.
- [S5] G. M. Sheldrick, *Acta Cryst. C*, 2015, **71**, 3.
- [S6] A. L. Spek, *J. Appl. Crystallogr.*, 2003, **36**, 7.